



LJMU Research Online

DAVIES, MJ, Taylor, Z, Ren, J, Leach, AG and Gibbons, P

Crystallisation of Aspirin via Simulated Pulmonary Surfactant Monolayers and Lung-Specific Additives

<http://researchonline.ljmu.ac.uk/id/eprint/6051/>

Article

Citation (please note it is advisable to refer to the publisher's version if you intend to cite from this work)

**DAVIES, MJ, Taylor, Z, Ren, J, Leach, AG and Gibbons, P (2017)
Crystallisation of Aspirin via Simulated Pulmonary Surfactant Monolayers and Lung-Specific Additives. Surface and Interface Analysis. ISSN 1096-9918**

LJMU has developed **LJMU Research Online** for users to access the research output of the University more effectively. Copyright © and Moral Rights for the papers on this site are retained by the individual authors and/or other copyright owners. Users may download and/or print one copy of any article(s) in LJMU Research Online to facilitate their private study or for non-commercial research. You may not engage in further distribution of the material or use it for any profit-making activities or any commercial gain.

The version presented here may differ from the published version or from the version of the record. Please see the repository URL above for details on accessing the published version and note that access may require a subscription.

For more information please contact researchonline@ljmu.ac.uk

<http://researchonline.ljmu.ac.uk/>

39 **1. Introduction**

40

41 Pain is associated with a number of well-documented disease states; including for example rheumatoid
42 arthritis, malignant disease and conditions of idiopathic origin [1]. Consequently, pain is a prevailing complaint
43 that presents worldwide and within the United Kingdom it is estimated that thousands of people experience
44 the issue on a daily basis [2]. The presentation of pain can result in a significant reduction in quality of life and
45 may affect socioeconomic function [3]. Pain management is routinely achieved through the administration of
46 analgesic medication via the oral, transdermal or parenteral routes. Although the more traditional routes of
47 analgesic drug delivery to the body hold merit (e.g. ease of use and dose flexibility) several drawbacks do exist
48 (e.g. discomfort at the injection site and variable bioavailability). Accordingly, interest in alternative, more
49 patient friendly methods to administer analgesic medication to the body has gained pace; one such example is
50 that of the inhaled route [4].

51 The lung serves as an effective portal for drug delivery to the body due to the large surface area for
52 absorption, the highly vascularised nature of the organ plus the thin, moist air-blood barrier [5]. The delivery
53 of particulate material to the respiratory tract is an inefficient process, with typically only 20% of the emitted
54 dose reaching the lung and contacting pulmonary surfactant [6]. This notable inefficiency may be ascribed to a
55 number of factors, including for example material cohesion / adhesion, particle size distribution along with
56 particle morphology [7]. Thus, in order to maximise the availability of drug substance for therapeutic benefit,
57 a formulation should exhibit the best possible combination of physicochemical characteristics (e.g. particle size
58 (optimal range between 1µm - 5µm), shape, crystal form, solubility, bioavailability and stability). Of
59 significance to the work presented herein, it is the morphology of the respirable material (and hence exposed
60 chemical functionalities) that will principally govern the interaction profile between an active pharmaceutical
61 ingredient (API) and pulmonary surfactant [8].

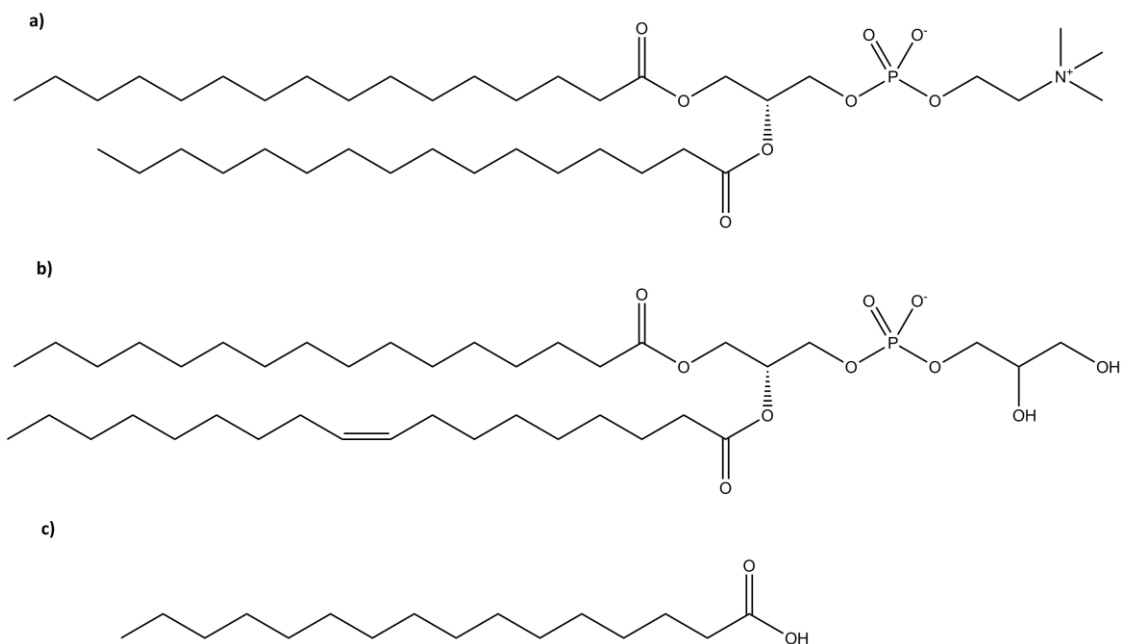
62

63

64

65 On delivery to the (deep) lung, an aerosolised formulation will initially interact with pulmonary surfactant
66 [9 & 10]. This material is a complex biological mixture that lines the inner surface of the lung (i.e. the alveolar
67 space) and reduces the surface tension term to maintain airway patency [11]. During the process of tidal
68 breathing, variation in pulmonary surfactant physical characteristics occurs [12], which can in turn influence
69 the processes of drug particle dissolution and subsequent absorption [13]. The principal components of
70 pulmonary surfactant are saturated dipalmitoylphosphatidylcholine (DPPC), unsaturated phosphatidylcholines,
71 phosphatidylglycerols (i.e. 1-palmitoyl-2-oleyl-sn-glycero-3-phosphatidylglycerol (POPG)) along with the
72 surfactant proteins (SP) A, B, C and D [14 & 15]. Absence of this endogenous material in new born infants
73 results in the precipitation of respiratory distress syndrome (RDS). This condition may be effectively managed
74 by the intratracheal administration of commercially available pulmonary surfactant replacement preparations
75 (i.e. Survanta®). Often such products are supplemented with palmitic acid (PA) to achieve a representative
76 lipid – protein profile. The chemical structures of DPPC, POPG and PA are presented in Figure 1.

77
78



79

80

81

82

83 **Figure 1.** The molecular structures of (a) DPPC, (b) POPG and (c) PA.

84

85

86

87

88 Langmuir monolayers may be applied within the laboratory setting to investigate the structure-function
89 activity of pulmonary surfactant [16, 17, & 18]. The experimental approach may also be exploited to stimulate
90 epitaxial nucleation and facilitate controlled crystal growth [19]. Here, the presence of an ordered two-
91 dimensional surface in proximity to a solubilised API can serve to reduce the activation energy necessary for
92 crystal nucleation when compared to similar homogenous media. As such, the model may be applied to
93 investigate the chemical complementarity between APIs / biologically relevant molecules at the alveolar air-
94 liquid interface. Indeed, the potential of Langmuir monolayers to stimulate crystal formation was successfully
95 demonstrated by Mu and co-workers during 2005, whereby the group employed DPPC monolayers to induce
96 and control glycine crystal development [20]. Various operating parameters were noted to influence resultant
97 crystal habits; including for instance the pH of the subphase and monolayer surface pressure. Flexibility in
98 operating conditions can thus afford the formulator with scope to achieve control over crystalline properties
99 (e.g. exposed surface chemistries).

100 Although Langmuir monolayers hold potential to inform understanding surrounding API nucleation and crystal
101 growth within simulated pulmonary environments, several drawbacks (e.g. low crystal yield plus large particle
102 size distribution) preclude use for industrial scale-up and patient end-use. Therefore, it is necessary to
103 investigate alternative routes of crystallisation, such as antisolvent crystallisation with biologically relevant
104 additives, to achieve controlled crystal growth and support chemical complementarity with appropriate yields.
105 The strategy involves the addition of a second solvent (i.e. ethanol) to a supersaturated, drug-containing
106 solution to reduce drug solubility and initiate crystallisation [21]. Typically, this approach is rapid and
107 generates a large number of micron-sized drug particles that are suitable for delivery to the (deep) lung. This
108 particular methodology was applied by Xie and co-workers in 2010, whereby a range of additives were used to
109 achieve control over drug crystal size and form [22]. Here, the group crystallised salbutamol sulphate in the
110 presence of compounds such as hydroxypropylmethylcellulose and demonstrated an influence on crystal
111 development, morphology and size distribution. The authors linked the findings to the capability of the
112 additives to interact favourably with specific chemical groupings on drug crystal surfaces and thus inhibit
113 growth.

114

115 Aspirin has been selected as the *model* API for study. This agent is administered extensively via the oral route
116 within the clinical setting to manage both acute pain and inflammation [23]. The molecule comprises of a
117 benzene ring, carboxylic acid and acetylated phenol groupings. Here, the intention is to obtain an improved
118 understanding as to how intrinsic chemical moieties within a drug molecule can influence the interaction with
119 lung-specific material (i.e. DPPC, POPG and PA) and thus govern crystal presentation.

120 Aspirin exerts its effect by irreversibly inactivating both the cyclo-oxygenase (COX)-1 and (COX)-2 enzyme
121 systems [24]. To date, the therapeutic compound has been subject to extensive investigation [25, 26, 27 &
122 28]. As such, aspirin is known to exist as two polymorphs (i.e. form I and form II) [25, 27 & 28]. Typically, form
123 I dominates, however in 2005 Vishweshwar and co-workers solved the structure for aspirin form II, both being
124 very similar in terms of internal molecular ordering [25, 26 & 29]. Aspirin form I exists with the monoclinic
125 space grouping of P21/c [28] having unit cell parameters of $a = 11.23(3)$, $b = 6.54(10)$, $c = 11.23(3)$ Å, $\beta =$
126 95.89° , $V = 821.218$ Å³ [28 & 30].

127 This study aims to investigate the crystallisation behaviour of aspirin when exposed to simulated pulmonary
128 surfactant monolayers and biologically relevant components of such. The work will provide an insight into the
129 morphologies of resultant aspirin crystals and enable the determination of important functionalities at the
130 dominant solid interfaces that may underpin the interaction with the alveolar air-liquid interface.

131
132
133
134
135
136
137
138
139
140
141
142
143
144

145 **2. Materials and Methods**

146

147 2.1 Materials

148

149 The starting material, aspirin with $\geq 99.0\%$ purity (Lot: 080M0092V), was purchased from Sigma-Aldrich, UK.

150 The surfactants DPPC (Avanti Polar Lipids, USA. Lot: 160PC-299), POPG (Avanti Polar Lipids, USA. Lot: 160-

151 181PG-113) and PA (Sigma-Aldrich, UK. Lot: 087K1877) were of analytical grade and used as supplied.

152 Chloroform (CHCl_3) (Sigma-Aldrich, UK) employed as the spreading solvent was of analytical grade ($\geq 99.9\%$).

153 Ethanol (HPLC grade, Sigma-Aldrich, UK) was used as the antisolvent in this work. Ultrapure water (Elga, UK),

154 demonstrating a resistivity of $18. \text{M}\Omega\text{cm}$, was used both during cleaning procedures and as the aqueous

155 subphase.

156 2.2 Methods

157

158 2.2.1 Aspirin Batch Crystallisation

159

160 A saturated solution of aspirin with a concentration of 7.5mg/ml was produced in 20ml of ultrapure water

161 heated to 40°C in a jacketed beaker connected to a circulating water bath (ThermoHaake DC10, USA) and

162 subsequently stirred at 700rpm . The solution was rapidly cooled in an ice bath to 1.5°C for an hour and a half

163 to facilitate crystallisation. The crystals were recovered via Buchner filtration and dried in an oven at 60°C

164 overnight. The resultant crystals were later analysed via scanning electron microscopy (SEM) and X-ray

165 diffraction (XRD).

166 2.2.2 Aspirin Antisolvent Crystallisation

167

168 A saturated solution of aspirin with a concentration of 100mg/ml was produced in 10ml of ethanol.

169 Subsequently, a total of 30ml of ultrapure water (i.e. the antisolvent) was heated to 20°C in a jacketed beaker

170 connected to a circulating water bath (ThermoHaake DC10, USA) and placed on a heating stage with a

171 magnetic stirrer. The aspirin solution was added drop wise to the ultrapure water with vigorous stirring. The

172 drug-containing solution was agitated for a period of 10 minutes. Resultant crystals were recovered via

173 Buchner filtration and dried in an oven at 60°C overnight. The approach was repeated with DPPC (1% and 5%),

174 POPG (1% and 5%) and PA (1% and 5%) in the aspirin solution.

177 The relatively low percentage strengths were chosen during this aspect of the study so as not to dominate the
178 crystallisation environment (i.e. as apparent in the Langmuir trough) and also align with budgetary constraints.

179 2.2.3 Langmuir Monolayers

180

181 Surfactant monolayers were produced using a Langmuir trough (Model 102M, Nima Technology, UK).
182 Surfactant free tissues (Kimtech Science, Kimberley-Clark Professional, 75512, UK) were soaked in chloroform
183 and used to clean all the glassware and contacting surfaces. Test runs that monitor surface pressure during
184 barrier compression were performed to ensure cleanliness. Trough cleanliness was confirmed at 0.4mN/m on
185 complete barrier compression, in the absence of a surfactant monolayer.

186 A spreading solution composed of DPPC, POPG and PA in the ratio 69:20:11 was produced by dissolving the
187 surfactant material in chloroform (1 mg/ml). In total, 10 μ l of this solution was delivered to the surface of the
188 pure water subphase by drop-wise addition using a Hamilton microsyringe and left for 10 minutes to facilitate
189 chloroform evaporation and surfactant spreading. The trough barriers were programmed to move to the
190 centre of the trough at a rate of 30cm²/min. Plots of surface pressure vs area per molecule (π -A) for the
191 surfactant system at 25°C were collected using a Wilhelmy plate at the centre of the compartment.

192

193 2.2.4 Aspirin Recrystallisation beneath Langmuir Monolayers

194

195 Recrystallisation was performed using a drug containing aqueous subphase at concentrations of 7.5mg/ml
196 aspirin at 25 \pm 1°C. The simulated pulmonary surfactant monolayer was compressed to surface pressures of
197 5mN/m or 50mN/m and left to stand for 16 hours to facilitate crystallisation. During collection, the inner
198 section of the Langmuir trough was isolated then the solid material was collected and subsequently filtered via
199 a Buchner filter.

200

201

202

203

204 2.2.5 Sample Characterisation
205

206 2.2.5.1 X-ray Diffraction (XRD)
207

208 To complete the XRD investigation, the aspirin crystals recovered from each system were mounted onto a
209 quartz sample holder. Diffraction patterns were obtained using Cu radiation ($\lambda = 1.54 \text{ \AA}$) at a voltage of 30 kV
210 and a current of 15 mA with an automatic, variable divergence slit (Rigaku Miniflex, Rigaku corporation, Japan).
211 Samples were scanned from 3° to $50^\circ 2\theta$. Subsequently, the data were compared with those presented in the
212 literature to characterise the solid form [27].

213

214 2.2.5.2 Scanning Electron Microscopy (SEM)
215

216 All samples were visualised via SEM analysis (Quanta 200 SEM, FEI, Holland). At the outset, the material was
217 palladium coated using a K550X sputter coater (EMITECH, UK) and then scanned using an acceleration voltage
218 of 10 kV at a working distance of approximately 10mm.

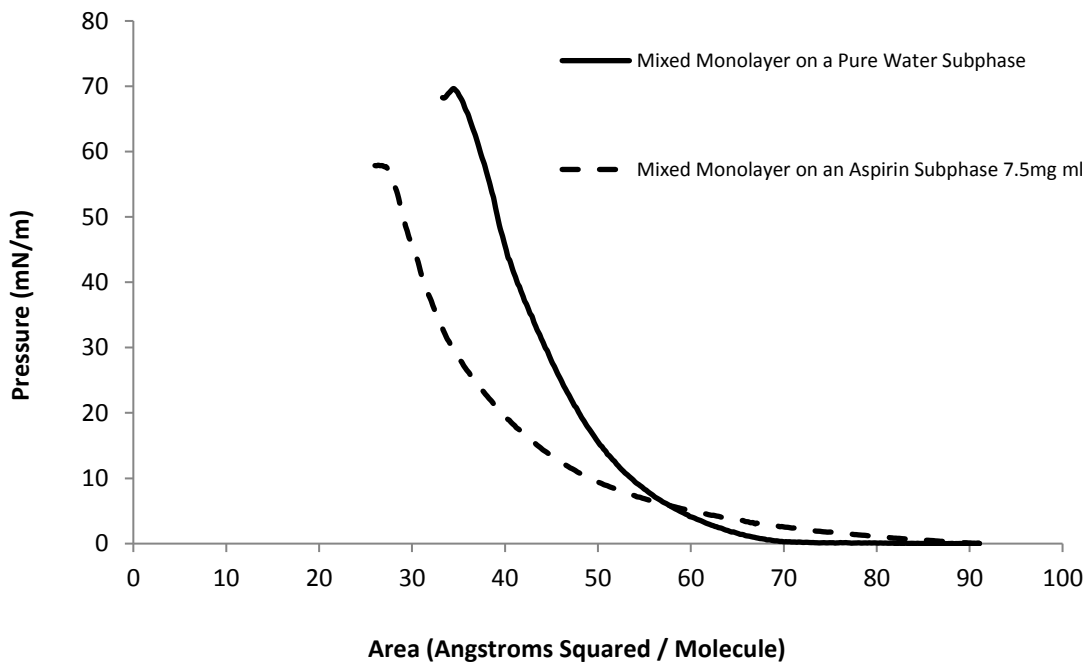
219 3. Results

220

221 3.1 Langmuir Monolayers
222

223 Langmuir pressure-area isotherms acquired for the mixed surfactant system when supported on either a pure
224 water or an aspirin containing subphase are presented in Figure 2. Upon inspection, it is evident that the
225 presence of the API within the supporting subphase did not adversely affect monolayer dynamics. Deviation
226 between each trace does confirm aspirin – simulated pulmonary surfactant interaction.

227



228

229 **Figure 2.** Langmuir π -A isotherms for the mixed surfactant systems at 25°C.

230

231 Distinct phase changes over the course of compression are denoted by the variation in recorded gradients
 232 within each trace. The limiting area per molecule for the mixed system in the absence of aspirin was
 233 approximately 55Å². However, further to the inclusion of aspirin within the subphase, the limiting area per
 234 molecule was estimated to be 42Å². The notable reduction in this term arises due to the interaction between
 235 those aspirin molecules in solution and the surfactant molecules forming the monolayer structure [19]. The
 236 result may be ascribed to the binding of drug molecules to the underside of the mixed surfactant monolayer,
 237 in turn forming a condensed ensemble.

238

239

240

241

242

243 3.2 Scanning Electron Microscopy

244

245 SEM images relating to aspirin crystals generated by various routes are presented in Figure 3. Crystalline
246 particles formed by conventional cooling crystallisation (Figure 3a) exhibited equant morphology and were
247 large in size (i.e. approximately $370\mu\text{m} \times 270\mu\text{m}$), thus precluding use for drug delivery to the lung. The
248 samples produced via mixed surfactant monolayers at surface pressures of 5mN/m (Figure 3b) and 50mN/m
249 (Figure 3c) displayed plate-like morphology, with bladed crystals being present in the sample generated at
250 50mN/m . In the case of both samples, the size of the resultant material would also not permit effective
251 delivery to the (deep) lung; indicative sizes being $90\mu\text{m} \times 140\mu\text{m}$ and $100\mu\text{m} \times 390\mu\text{m}$, respectively.

252 With respect to the material produced via antisolvent crystallisation, the particle size was significantly smaller.
253 Antisolvent crystallisation in the absence of additives produced drug crystals of an irregular nature, which may
254 be attributed to limited control over the crystallisation process (data not shown). The inclusion of lung-specific
255 additives had a profound impact upon crystal size distribution and morphology. In terms of antisolvent
256 crystallisation in the presence of DPPC 5% (Figure 3d), the crystalline material had a relatively smooth texture
257 with the sample containing particulates demonstrating cohesive properties. Here, the typical size range was
258 $35\mu\text{m} \times 45\mu\text{m}$. In terms of the material obtained via antisolvent crystallisation in the presence of POPG 5%
259 (Figure 3e), plate-like morphology was apparent with some deviation in the size distribution; the
260 representative particle size was estimated at $90\mu\text{m} \times 55\mu\text{m}$. Clearly, within this particular sample the particles
261 were larger when compared to those obtained with DPPC as the lung-specific additive. Once again, the
262 particles demonstrated cohesive properties with agglomerates clearly visible. The inclusion of PA at 5% (Figure
263 3f) within the antisolvent reaction vessel once more resulted in the generation of small drug-containing
264 particulates similar to the DPPC sample; here, the typical size was $35\mu\text{m} \times 45\mu\text{m}$. Within this sample plate-like
265 crystals with smooth surfaces were evident. Overall, the data indicate that antisolvent crystallisation, in
266 combination with lung-specific additives, resulted in the presentation of drug-containing particulates that
267 demonstrated plate-like morphology at geometric diameters within the 10's of micron size range. The route of
268 crystallisation governed the crystal habit.

269

270

271
272
273
274
275
276
277
278
279
280
281
282
283
284
285
286
287
288
289
290
291
292
293
294
295
296
297
298

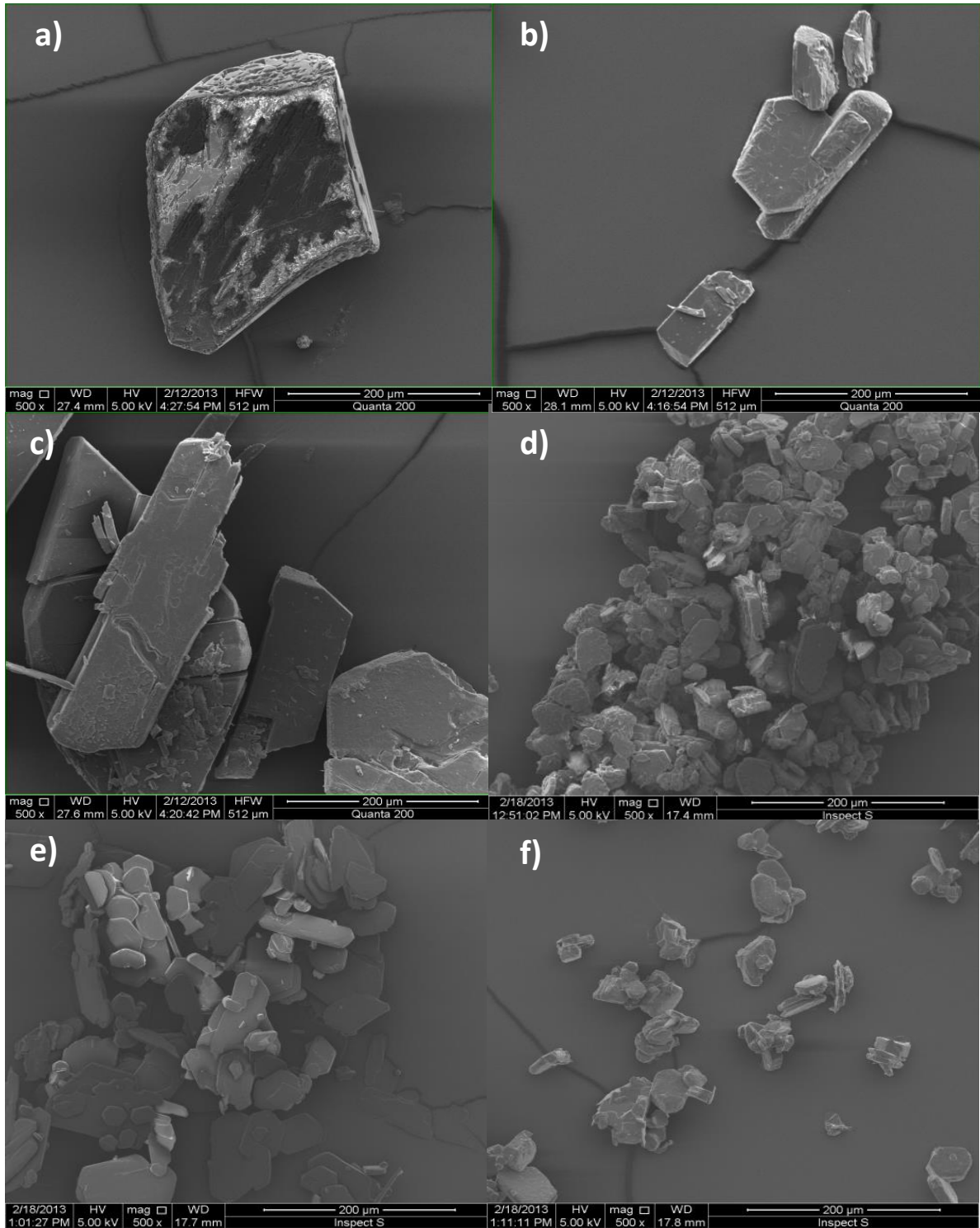
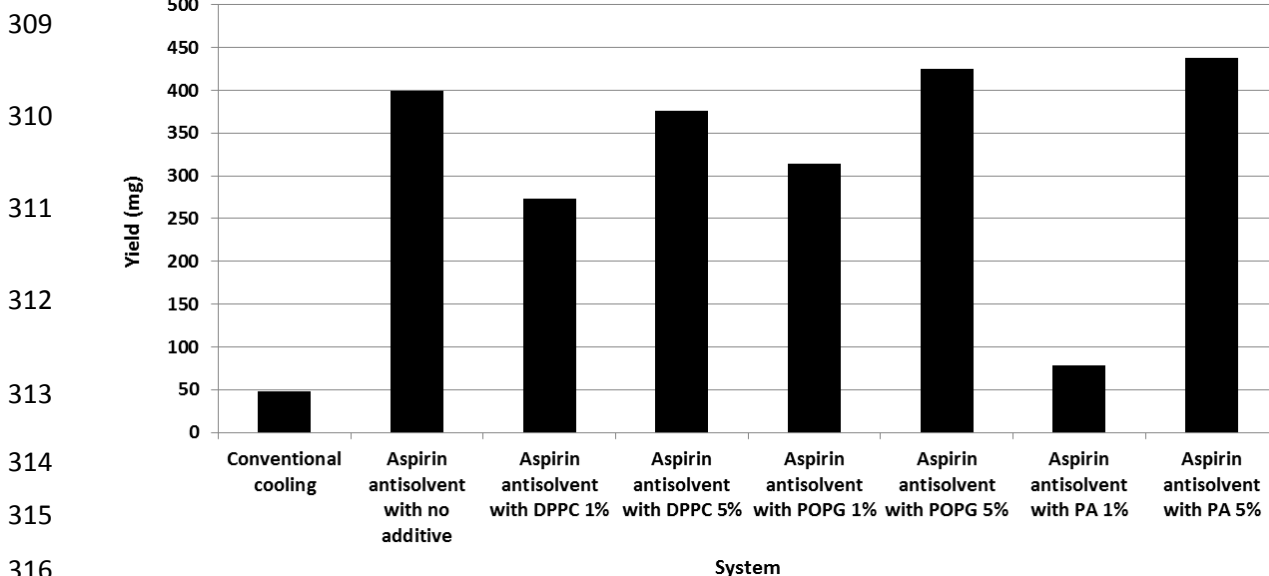


Figure 3. SEM images of aspirin crystals produced under various study conditions: a) conventional cooling crystallisation, b) mixed monolayer at 5mN/m, c) mixed monolayer at 50mN/m, d) antisolvent crystallisation with DPPC 5%, e) antisolvent crystallisation with PPOG 5% f) antisolvent crystallisation with PA 5%. Typical morphologies included equant and plate-like. The crystallisation environment dictated gross particle morphology.

299 3.3 Crystal Yield

300

301 Crystal yield data from the various systems under investigation are presented in Figure 4. Upon inspection of
302 the data it is evident that the conventional cooling approach resulted in the smallest crystal yield. This result
303 may be ascribed to the limited solubility of aspirin in ultrapure water under the predefined experimental
304 conditions and confirms this route of crystal manufacture would be unsuitable at the industrial scale. The
305 application of antisolvent crystallisation with lung-specific additives resulted in the generation of a greater
306 crystal mass, which may be attributed to the increased capacity for drug solubilisation within each system. As
307 the concentration of each specific additive was increased, the yield from each antisolvent system also
308 increased.



317 **Figure 4.** Crystal yield data from the systems under investigation. The inclusion of lung-specific additives at higher
318 percentages increased the crystal yield.

319

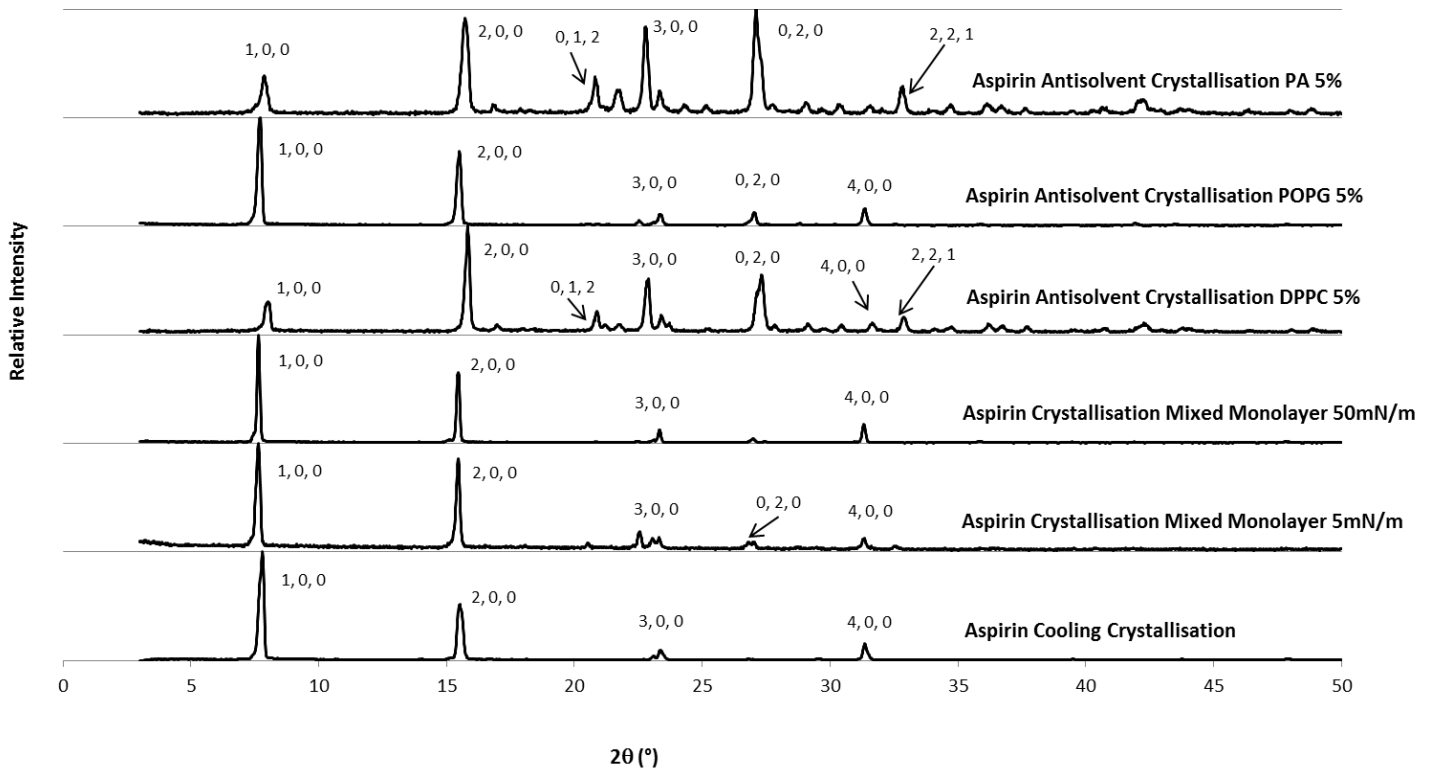
320 Inhibition of crystal growth was most notable in the case of antisolvent crystallisation in the presence of PA at
321 the 1% level, with 78.7mg of material generated. Conversely, antisolvent crystallisation in the presence of PA
322 at 5% concentration resulted in the largest recorded yield. Of particular note is the mass obtained from the
323 antisolvent crystallisation POPG 5% system. Here, a relatively large amount of drug-containing crystalline
324 material (i.e. 424.7mg) was recovered. Interestingly, the XRD diffraction pattern for this particular sample
325 reflected that obtained from the crystalline material obtained from the mixed surfactant monolayers at
326 5mN/m and 50mN/m.

327 3.4 X-ray Diffraction Analysis

328

329 The crystalline material recovered from each system under investigation was subject to XRD examination;
330 representative traces are illustrated in Figure 5. Analysis was conducted on 'as synthesised' samples, such that
331 dominance within the morphology could be determined; this approach has been applied in previous crystal
332 elucidation studies [31 & 32]. All intensity values were converted to relative values (e.g. percentages) to
333 highlight subtle changes in aspirin morphology under variable experimental conditions.

334



344

345 **Figure 5.** XRD analysis of aspirin crystals recovered from each system under investigation. The route of crystallisation
346 holds a significant bearing on the material acquired from each system. With the Langmuir trough crystallisation
347 environment in mind, similarity is most evident in the case of the antisolvent system with POPG at the 5% level. Thus, the
348 data indicate that the latter route of particle manufacture would be most suitable for material scale up to ensure internal
349 lung surface complementarity.

350

351

352

353

354 The diffraction data highlight that there is a clear difference between the aspirin crystals produced under pre-
355 determined conditions. The preferred orientation noted reflects the area of the face on which the crystals are
356 lying and the morphology of the material. With respect to the conventional cooling sample, the (200) face
357 demonstrates a reflection of 52%, with the (300) and (400) facets showing reflections of 10% and 15%,
358 respectively; the XRD pattern matches those previously determined for single aspirin crystals [28]. The XRD
359 profile of the as synthesised sample by antisolvent crystallisation with PA 5% is comparable to the XRD pattern
360 for ground sample [32], this reflecting the size and morphology of the crystal.

361 The XRD patterns for the other systems show a clear difference in preferred orientation, which to a certain
362 extent reflects the difference in the morphology [31]. As anticipated, the dominant reflection presenting
363 within the sample produced via the conventional cooling method was the (100) facet. This particular reflection
364 is expected to govern the crystal morphology of aspirin form I because the material was grown in water and is
365 assigned a space grouping of P21/c [27 & 28]. The (100) reflection within the sample was applied to confirm
366 the remaining faces associated with the material. Here, additional readings at 2θ values of 15.81° , 23.83° and
367 31.9° suggest the presence of the (200), (300) and (400) reflections, respectively [27].

368 The XRD data acquired from the mixed monolayer system at 5mN/m demonstrates dominance in the (100)
369 reflection. This result may be ascribed to the conditions under which the crystals were allowed to grow (i.e. an
370 aqueous environment). An interesting point to note with this sample is the increase in percentage intensity
371 associated with the (200) face when compared to the cooling crystallisation sample. Here, the reflection
372 demonstrates 85% which represents a 23% increase. With regard to the crystalline aspirin sample acquired
373 from the mixed surfactant system at 50mN/m, it is apparent that close similarity exists with that obtained
374 from the lower surface pressure. That is to say, the (100) facet dominates the situation with the (200)
375 reflection being a close second. In this case, the (200) reflection presents with a 65% intensity, this figure
376 being 13% greater than the conventional cooling sample. The data suggest that the mixed surfactant
377 monolayers, at both low and high surface pressures, influence the reflection of the (200) face and as such this
378 face, with associated external chemistries, may indeed be important during the interaction with endogenous
379 pulmonary surfactant.

380 The XRD analysis for aspirin crystals recovered from the antisolvent crystallisation system with DPPC 5% as a
381 lung-specific additive indicate that a number of reflections present (i.e. a random array of peaks are evident).
382 Here, the (100) facet presents at 30%, the (200) face at 100%, (300) plane at 51% and (400) plane at 11%
383 relative intensity. The application of DPPC at 5% within the antisolvent reaction vessel does not permit
384 effective control over particle morphology to reflect the simulated pulmonary surfactant systems. On
385 inspection of the XRD data for the crystalline material produced with POPG 5% as the lung-specific additive, it
386 is clear that similarity exists between the diffraction data acquired for the simulated pulmonary surfactant
387 systems at high and low surface pressure. We suggest, therefore, that this integral component of endogenous
388 pulmonary surfactant would be suitable to guide the presentation of aspirin crystals complementary to the
389 internal surface of the (deep) lung. Conversely, the inclusion of PA at the 5% level within the reaction vessel
390 did not favour the production of crystalline particles demonstrating similar diffraction patterns to the mixed
391 monolayer systems. In this case, the (100) reflection intensity diminished, whilst the (200), (300) and (020)
392 reflections dominated within the morphology. Overall, the XRD data confirm that lung-specific additives can
393 influence the synthesis of aspirin during the process of antisolvent crystallisation. Thus, in order to rationally
394 engineer drug-containing particulates to support interaction with internal lung surfaces, the manufacturing
395 process and additive must be carefully defined.

396

397 **3 Discussion**

398

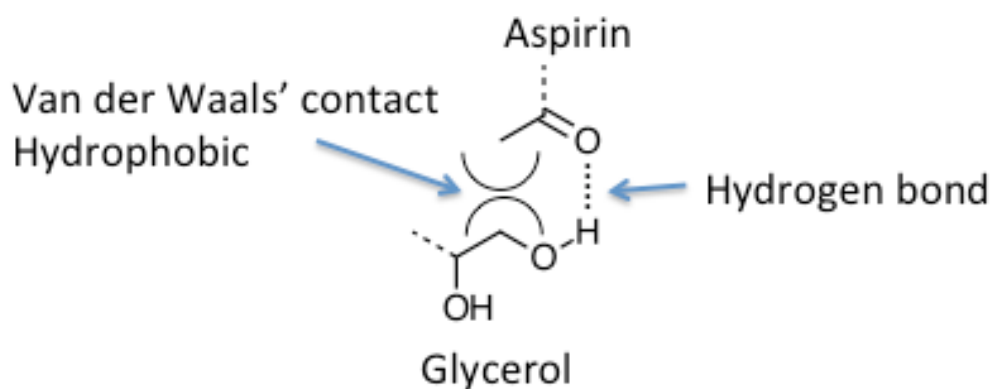
399 During this work stable, simulated pulmonary surfactant monolayers were generated using DPPC, POPG and
400 PA. We have previously detailed how the protrusion of related chemical functionalities into the supporting
401 subphase may attract solubilised APIs and correspondingly reduce the activation energy required for
402 crystallisation [8 & 18]. In order to better understand the crystallisation mechanism(s) associated with aspirin
403 when in contact with simulated pulmonary surfactant monolayers or components thereof, consideration must
404 be given to the underlying chemistries that govern the initial interactions between each species.

405

406

407 DPPC is a zwitterionic molecule that contains anionic hydrogen bond acceptors and a cationic ammonium
408 group. The latter, which is at the termini and therefore exposed most prominently to the aqueous layer, has
409 the potential to form strong interactions with aspirin molecules dissolved in solution. In particular, the
410 carboxylate group arising from the dissociation of aspirin in water will associate with the ammonium group via
411 charge-charge interaction. The polarised CH bonds of the methyl groups in the ammonium group may also
412 interact through specific binding interactions with the carboxylate or other hydrogen bond acceptors in the
413 aspirin. This functionality will therefore interact most favourably with the (100) face which presents the
414 carboxylate group. By contrast, the POPG retains the phosphate oxygens but has the hydrogen bonding
415 features of the glycerol group in place of the charged features of the ammonium group in DPPC. These groups
416 are much better placed to interact with the acetyl group of aspirin with which they can form polar and
417 hydrophobic interactions. This amphiphilic behaviour is one of the defining characteristics of glycerol that
418 underpins its utility in stabilising many compounds during their crystallisation. The proposed mechanism for
419 interaction between the species considered herein is presented in Figure 6. The PA molecule will primarily
420 present carboxylate on the lower surface of the monolayer and is therefore unlikely to interact constructively
421 with aspirin.

422



424

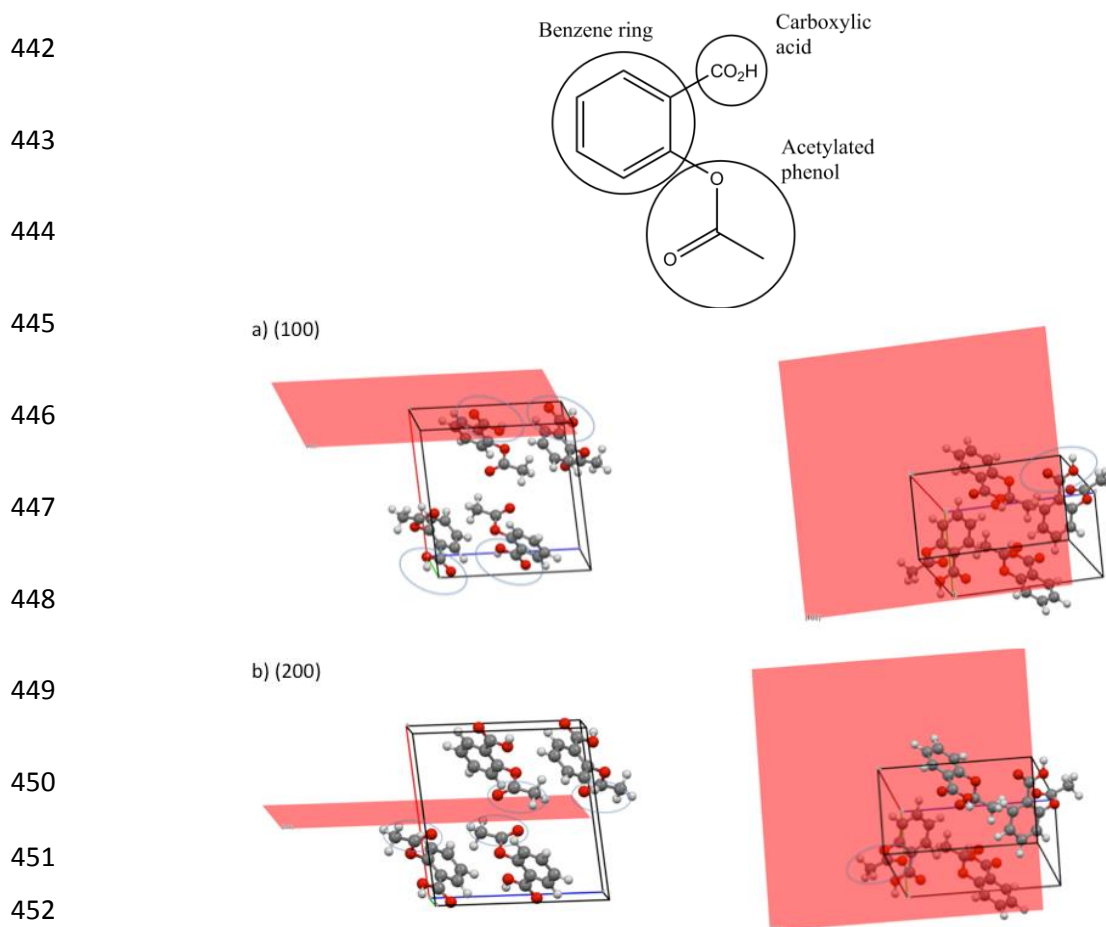
425 **Figure 6.** *The proposed mechanism of interaction between key aspirin and POPG functionalities within the simulated*
426 *pulmonary surfactant system.*

427

428

429

430 With respect to aspirin crystals formed beneath the simulated pulmonary surfactant monolayers at 5mNm^{-1}
431 and 50mNm^{-1} , it is clear that the (100) and (200) planes dominate the scenario. A similar trend was also noted
432 in the case of those aspirin crystals recovered from the rapid cooling crystallisation vessel, although in this
433 particular case the (200) plane was less prominent. The data confirm that both crystal faces, and associated
434 chemistries, are important during material synthesis. The principal crystal faces identified via XRD analysis
435 were visualised using the Mercury v3.0 software package. Here, the (100) face predominately involves the
436 carboxylic acid group. As illustrated in Figure 7 panel a, this group is positioned across this face in a way that
437 will maximise interactions between the carboxylic acid and solvent water. The related (200) face, illustrated in
438 Figure 7 panel b, is dominated by the acetyl group. Specifically the carbonyl oxygen and the hydrophobic
439 methyl group are presented. This pair of groups is likely to form attractive interactions with the glycerol head
440 groups of the surfactant molecules, as shown in Figure 1. Glycerol is known to interact amphiphilically in this
441 way [33].



453 **Figure 7.** The chemical structure of aspirin with key functionalities along with their presentation at the dominant (100) and
454 (200) crystal planes.

455 When considering drug particle delivery to the (deep) lung, the physicochemical changes associated with
456 pulmonary surfactant during tidal breathing are of importance. This is so because on initial contact with
457 internal surfaces in the (deep) lung, respirable drug-containing particles are wetted by pulmonary surfactant
458 and the related hypophase then subsequently displaced towards the alveolar epithelium [11 & 13]. The extent
459 of particle immersion is dependent on the surface pressure of the surfactant monolayer, with greater
460 immersion apparent at a lower surface pressure [13]. During inhalation, the surface area of the alveoli
461 increases, which leads to a related decrease in surfactant surface pressure; the net effect being lack of
462 uniformity of the constituent molecules and the availability of polar head groups for interaction. Conversely,
463 during exhalation the alveolar surface area decreases and a related increase in the surfactant surface pressure
464 is noted. This effect results in a more ordered scenario whereby the hydrocarbon chains of the surfactant
465 molecules are fully extended towards the alveolar lumen and the polar heads groups associate strongly with
466 the supporting aqueous subphase. At this point, both the polar head groups and pulmonary hypophase are
467 theoretically 'hidden' from descending drug particles.

468 With this in mind, during the breath holding stage of the accepted inhaler technique, rationally engineered
469 drug-containing particulates may descend upon a pulmonary surfactant monolayer that is in the gaseous
470 phase and interact with the polar head groups effectively. Here, we suggest that the extent of particle wetting
471 and related immersion would be greater; hence, the time lag to reach the systemic circulation would be
472 reduced leading to more effective systemic presence and related disease treatment (i.e. pain management).
473 With commercially available respirable formulations in mind, there is no guarantee that such preferred
474 external chemistries between a drug particle and pulmonary surfactant will come into contact, in effect the
475 association between each species is essentially uncontrolled.

476

477

478

479

480 In general, drug particle manufacture within the pharmaceutical industry is often conducted via crude,
481 uncontrolled crystallisation processes that typically utilise organic solvents. Further to crystallisation, a drug-
482 containing suspension is typically filtered, dried and subjected to comminution procedures. Such stages can
483 be costly, time consuming, inefficient and can have significant effects on powder stability, flow properties,
484 energetics and may go so far as to destabilise the crystal structure [34]. As such, alternative methods for
485 respirable particle manufacture have been investigated, for example spray drying [35]. Although this
486 particular method is a one-step manufacturing process, the high temperatures that are often used prove
487 restrictive for thermally liable compounds and often lead to amorphous particle generation [36]. As a result of
488 such inherent drawbacks, attention is now focussed on alternative crystallisation techniques that involve single
489 step particle production leading to material with narrow size distribution, optimal aerodynamic parameters
490 and desirable surface properties, a prime example of this is antisolvent crystallisation.

491 In 2012 Park and Yeo successfully applied antisolvent crystallisation to synthesise carbamazepine-containing
492 particulates [21]. Here, the authors considered a wide range of experimental parameters during particle
493 generation such as solution concentration, crystallisation temperature, solution addition rate and the
494 application of ultrasound. The data indicated that as the concentration of the carbamazepine solution was
495 increased the resultant particle size decreased, which also held true when the temperature of the system was
496 increased. Importantly, the group noted that smaller drug-containing particles were generated with rapid
497 introduction of the antisolvent (10ml/min) compared to larger particles with slower introduction (1.4ml/min);
498 the average particle size range was reported to be 62.1 μm – 112.3 μm , respectively. Moreover, the rate of
499 antisolvent addition did not influence the crystal habit; hence, exposed chemical moieties remained constant.
500 Thus, the authors demonstrate that antisolvent crystallisation can provide a route to manufacture drug-
501 containing particulates within a narrow particle size range at the 10's of micron scale.

502

503

504

505

506

507 **4 Conclusion**

508

509 This study has provided opportunity to better understand the crystallisation behaviour of the commonly
510 prescribed analgesic agent aspirin when in contact with material located at the alveolar air-liquid interface.
511 Key crystal planes for consideration during the interaction with simulated pulmonary surfactant, and
512 components thereof, include the (100) and (200) facets. Here, we have demonstrated that the crystallisation
513 environment (i.e. heterogeneous nucleating surface vs antisolvent crystallisation) and the presence of
514 additives are important in guiding the morphology of drug-containing particulate material. The understanding
515 gained may be applied in the rational engineering of drug-containing respirable particulates for local or
516 systemic disease management.

517 Whilst this exploratory study (i.e. the combination of unrelated crystallisation techniques to better understand
518 drug chemical complementarity with the lung) was conducted under ambient conditions, potential exists to
519 execute such work under physiologically relevant parameters via application of the lung biosimulator [37].
520 This new development within the field of Langmuir monolayer technology also provides the user with scope to
521 investigate the impact of environmental toxins (e.g. cigarette / e-cigarette / cannabis smoke) on lung function
522 [38]. Moreover, the approach has application in the dissolution profiling of orally inhaled products (OIPs)
523 along with the implementation of *in vitro* – *in vivo* correlation studies.

524

525 **5 Acknowledgements**

526 MJD would like to thank LJMU for funding this research project. Special thanks go to Mr Paul Burgess and Mr
527 Geoffrey Henshaw for technical support throughout.

528

529

530

531

532 **6 References**

- 533 1. Sherwood, L. (2010). Human Physiology: From Cells to Systems. Seventh Edition. Brooks / Cole Cengage
534 Learning, United States of America.
- 535 2. The British Pain Society. (2016). <http://www.britishpainsociety.org/>.
- 536 3. NHS Quality Improvement Scotland. (2008). Getting to GRIPS with Chronic Pain in Scotland Second Edition.
- 537 4. Farr, S.J., Otulana, B.A. (2006). *Advanced Drug Delivery Reviews*. **58**, 1076-1088.
- 538 5. Michael E. Aulton and Kevin M.G. Taylor. (2013). Churchill Livingstone, China.
- 539 6. Chrystyn, H. (2001). *British Journal of Clinical Pharmacology*. **51(4)**, 289–299.
- 540 7. Davies, M.J., Brindley, A., Chen, X., Doughty, S.W., Marlow, M., Shrubbs, I. & Roberts, C.J. (2005).
541 *Pharmaceutical Research*. **22(7)**, 1158 - 1166.
- 542 8. Davies, M.J., Kerry, T.D., Seton, L., Murphy, M.F., Gibbons, P. Khoo, J. & Naderi, M. (2013). *International*
543 *Journal of Pharmaceutics*. **446**, 34-45.
- 544 9. Schleh, C., Kreyling, W. G., & Lehr, C-M. (2013). *Particle and Fibre Toxicology*. **10**, 6.
- 545 10. Arora, S., Kappl, M., Haghi, M., Young, P. M., Traini, D. & Jain, S. (2016). *RSC Advances*. **6**, 25789-25798.
- 546 11. Notter, R.H. (2000). Lung Surfactants: Basic Science and Clinical Applications; Marcel Dekker: New York,
547 United States of America.
- 548 12. Davies, M.J., Brindley, A., Chen, X., Doughty, S.W., Marlow, M., Roberts, C.J. (2009). *Colloids and Surfaces B:*
549 *Biointerfaces*. **73**, 97-102.
- 550 13. Schürch, S., Geiser, M., Lee, M.M., Gehr, P. (1999). *Colloids and Surfaces B: Biointerfaces*. **15**, 339-353.
- 551 14. Goerke, J. (1998). *Biochim Biophys Acta*. **1408**, 79-89.
- 552 15. Bringezu, F., Pinkerton, K.E., Zasadzinski, J. (2003). *Langmuir*. **19**, 2900-2907.
- 553 16. Giner-Casares, J. J., Brezesinski, G. & Möhwald, H. (2014). *Current Opinion in Colloid & Interface Science*.
554 **19**, 176–182.
- 555 17. Stefaniu, C., Brezesinski, G. & Möhwald H. (2014). *Advances in Colloid Interface Sciences*. **208**, 197-213.
- 556 18. Davies, M.J., Seton, L., Tiernan, N., Murphy, M.F. & Gibbons, P. (2011). *International Journal of*
557 *Pharmaceutics*. **421**, 1–11.
- 558 19. Choudhury, S., Bagkar, N., Dey, G.K., Subramanian, H., Yakhmi, J.V. (2002). *Langmuir*. **18**, 7409-7414.

- 559 20. Mu, Y-D., Xiao, F., Zhang, R-J., Li, H-Y., Huang, W., Feng, X-S., Liu, H-G. (2005). *Journal of Crystal Growth*.
560 **284**, 486-494.
- 561 21. Park, M. & Yeo, S., (2012). *Chem Eng Res Des*. **90**, 2202-2208.
- 562 22. Xie, S., Poornachary, S.K., Chow, P.S., & Tan R.B.H. (2010). *Crystal Growth Design*. **10**, 3363–3371.
- 563 23. BNF 71: British National Formulary 71. (2016). *British Medical Association & Royal Pharmaceutical Society*
564 *of Great Britain*.
- 565 24. Rang, H.P., Dale, M.M. (2007). Rang and Dale's Pharmacology, Sixth Edition. Churchill Livingstone Elsevier,
566 United Kingdom.
- 567 25. Bond, A.D., Boese, R. & Desiraju, G.R. (2007). *Angewandte Chemie International Edition*. **46**, 618-622.
- 568 26. Bond, A.D., Boese, R. & Desiraju, G.R. (2007). *American Pharmaceutical Review*. **May / June**, 1-4.
- 569 27. Aubrey-Medendorp, C., Parkin, S. & Li, T. (2008). *Journal of Pharmaceutical Sciences*. **97(4)**, 1361-1367.
- 570 28. Bond, A.D., Solanko, K.A., Parsons, S., Redder, S. & Boese, R. (2011). *Crystal Eng Comm*. **13**, 399-401.
- 571 29. Vishweshwar, P., McMahon, J. A., Oliveira, M., Peterson, M. L. & Zaworotko, M. J. (2005). *Journal of the*
572 *American Chemical Society*. **127(48)**, 16802–16803.
- 573 30. Allen, F.H., (2002). *Acta Cryst*. **B58**, 380–388.
- 574 31. Morris K.R., Schlam R.F., Cao W. & Short M.S. (2000). *Journal of Pharmaceutical Sciences*. **89(11)**, 1432-
575 1442.
- 576 32. Jain H., Kailas S. Khomane K. S. & Bansal A. K. (2014). *Cryst Eng Comm*. **16**, 8471-8478.
- 577 33. Vagenende, V., Yap, M.G. & Trout, B.L. (2009). *Biochemistry*. **48(46)**, 11084-11096.
- 578 34. Shekunov, B.Y. & York, P. (2000). *Journal of Crystal Growth*. **211**, 122-136.
- 579 35. Vehring, R. (2008). *Pharmaceutical Research*. **25(5)**, 999-1022.
- 580 36. Chioua, D. & Langrish, T. A. G. (2007). *Drying Technology: An International Journal*. **25(9)**, 1427–1435.
- 581 37. Davies, M.J. (2014) International patent application: WO2014199178. Device and method for simulating
582 pulmonary environments.
- 583 38. Davies, M.J., Birkett, J.W., Kotwa, M., Tomlinson, L. & Woldetinsae, R. (2017). Surface and Interface
584 Analysis. DOI: 10.1002/sia.6205.
- 585